

Cite as:

Peng C, Xiang Y, Huang W, Feng Y, Tang Y, Biljecki F, Zhou Z (2025): Measuring the value of window views using real estate big data and computer vision: A case study in Wuhan, China. *Cities*, 156: 105536.

Measuring the value of window views using real estate big data and computer vision: a case study in Wuhan, China

Chucui Peng ^{a,b}, Yang Xiang ^a, Wenjing Huang ^a, Yale Feng ^a, Yongqi Tang ^a, Filip Biljecki ^{b,c}, Zhixiang Zhou ^{a,*}

^a College of Horticulture and Forestry Sciences / Hubei Engineering Technology Research Center for Forestry Information, Huazhong Agricultural University, China

^b Department of Architecture, National University of Singapore, Singapore

^c Department of Real Estate, National University of Singapore, Singapore

***Corresponding author:** Zhixiang Zhou, College of Horticulture and Forestry Sciences, Huazhong Agricultural University, Hongshan district, Wuhan 430070, PR China (whzhouzx@mail.hzau.edu.cn, whzhouzx@126.com)

Abstract

Window views significantly influence residential quality and real estate value, particularly in high-rise residential buildings. Previous studies have predominantly focused on water and green views, resulting in a lack of clarity regarding the influence of other types of views on house prices. In this study, we quantified and analyzed the impacts of 9 window view elements, including sky, high-rise buildings, low-rise buildings, trees, grass, water, hard ground, roads, and barren land, on housing prices using online real estate images and computer vision techniques. Focusing on high-rise buildings constructed in the past five years, our findings, based on spatial hedonic pricing models, reveal that an increased proportion of water views through windows has a significant positive effect on property prices. Conversely, the presence of grass and hard ground is associated with significant negative impacts. This study examines the influence of various window view elements on apartment prices, offering valuable insights for urban planning, architectural design, and property development.

Keywords: High-density cities; Window views; Computer vision; Real estate value; Hedonic price model; SHapley Additive exPlanations

1. Introduction

Modern urban dwellers spend approximately 80-90% of their time in enclosed buildings (Park and Nagy, 2018). Consequently, windows acquire critical importance for both the physical and mental health of occupants, serving as a bridge between indoor and outdoor landscapes (Elsadek et al., 2020), providing visual, auditory, and tactile sensory stimulation (Hasegawa et al., 2022), and facilitating a connection with nature (Schmid and Säumel, 2021; Sheng et al., 2024). The quality of window views is pivotal in urban sustainability, influencing neighborhood contentment, health and well-being, architectural design, and urban planning. For example, high-quality window views are deemed effective in increasing residents' satisfaction and alleviating loneliness (Chang et al., 2020; Bi et al., 2022), lessening stress and improving concentration in students (Li and Sullivan, 2016; Lindemann-Matthies et al., 2021; Vásquez et al., 2019), reducing discomfort among office workers (Aries et al., 2010), and improving mental health recovery, thereby expediting recuperation rates in hospital patients (Ulrich, 1984; Raanaas et al., 2012).

The expansion of urban areas has led to a significant influx of populations into cities, intensifying challenges related to land scarcity and demographic pressures. To accommodate these growing populations, high-density urban environments often rely on the construction of high-rise buildings, perceived as a more “sustainable” solution (Wang and Shaw, 2018). However, high-rise buildings may isolate residents from green spaces, reducing their access to nature and creating an inequitable distribution of green space (Elsadek et al., 2020). This phenomenon also holds for views from windows, as buildings in high-density cities are characterized by tall upper floors, high street canyon height-to-width ratios, and high floor area ratios (Biljecki and Chow, 2022). Consequently, apartments in high-density cities have vastly different views from windows depending on the floor, location, and other factors (Li et al., 2022). Some studies have explored the influence of window view elements at smaller scales, such as campuses, hospitals, and individual neighborhoods (Lin et al., 2022; Raanaas et al., 2012; Hasegawa et al., 2022; Schmid and Säumel, 2021), the link between different landscapes and window views at the urban scale and encompassing a variety of scenarios remains to be further explored.

The view through a window can influence the value of real estate, which has been confirmed by numerous hedonic price studies based on the real estate market (Sander and Polasky, 2009; Yamagata et al., 2016). However, there is significant variation in the attention given to different landscape elements. The focus of the majority of studies lies

on water views and green views, which have been shown to command higher premiums for residences with views of water and greenery (Luttik, 2000; Jim and Chen, 2006; Jim and Chen, 2009; Yamagata et al., 2016; Wu et al., 2022). Although some studies have employed street view images to measure the visibility of buildings and the sky, assessing their impact on housing prices (Yang et al., 2023; Qiu et al., 2022), the representation of buildings and sky visibility in street environments does not equate to that from high-rise residential window views. Consequently, the roles that the sky, buildings, and more infrequent landscapes like roads, grass, and barren land play in window views in high-density cities warrant further investigation.

Addressing the limitations of previous studies, and taking Wuhan as a case study, our research obtains real window view images of high-rise residential buildings from a real estate online platform. Using computer vision, we aim to accurately segment the window view images of apartment samples and analyze the indices of 9 window view elements, including sky, high-rise buildings, low-rise buildings, grasses, hard ground, trees, water, roads, and barren land. Based on this approach, we intend to explore their effects on apartment prices using spatial hedonic price models, while simultaneously focusing on nonlinear relationships through the application of XGBoost regression and SHapley Additive exPlanations (SHAP) methods. Specifically, we seek to expand this area of inquiry by exploring the following two questions:

1. How can we obtain urban-scale window view data of high-rise residential buildings and construct a workflow for semantic segmentation?
2. How do different window view elements impact the prices of high-rise residential apartments in Wuhan?

2. Literature review

2.1 Quantitative evaluation of window views

Representing window views through quantitative methods is an essential prerequisite for incorporating window views into mathematical models. Earlier researchers primarily utilized dummy variables to represent window views. After reviewing 35 papers published between 1973 and 2003 that quantified the impact of views on housing prices using dummy variables, Bourassa et al. (2004) found that most of these studies only examined the influence of water views, while other types of landscapes were largely neglected. Therefore, they chose to simultaneously investigate the impact of

water views, other views, and the appearance of landscaping in the neighborhood on housing prices. Similarly, Jim and Chen (2006, 2009) investigated the impact of window views on real estate values in Guangzhou and Hong Kong, employing dummy variables for green views, mountain views, and water views, respectively. In recent years, Li et al. (2020) determined that a window view of a polluted river diminishes house prices, by using a dummy variable for river visibility. Potrawa and Teterewa (2022) employed deep learning to recognize window views. They also used dummy variables to represent landscapes. However, the dummy variable merely quantifies the presence or absence of a landscape and fails to measure the proportion of the landscape outside the window. Additionally, this method only describes rarer landscapes, posing challenges in quantifying common landscapes like buildings and sky.

The development of Geographic Information System (GIS) has introduced a novel approach to quantifying window views. Numerous studies have quantified landscape visibility employing digital elevation modeling (DEM) alongside visual field analysis (Sander and Polasky, 2009; Mittal and Byahut, 2019; Dai et al., 2023). Acknowledging that DEM data may ignore the height of buildings and landscapes (Mistick et al., 2023), some researchers developed a digital surface model (DSM) to assess a property's view using LiDAR (Hamilton and Morgan, 2010). Yamagata et al. (2016) further incorporated aerial photos to quantify the window view of Yokohama Bay. While GIS-based viewshed analysis effectively analyzes landscape visibility at a larger scale, Yamagata et al. (2016) also noted that visibility does not fully represent visual quality, which is significantly influenced by structure, color, and contrast.

The emergence of city information models (CIM) has enabled high-precision reproduction of window views (Li and Samuelson, 2020). Turan et al. (2021) quantified the effects of daylight and views on office rents through ray tracing and a 3D model of Manhattan. Li et al. (2022) employed 3D CIM to batch-generate window views of buildings in the model and quantified the window views using semantic segmentation. Swietek and Zumwald (2023) expanded the assessment of visual capital across Switzerland on a building-by-building basis. However, considering that not every city has an available CIM, this approach continues to exhibit specific constraints. Moreover, this method's limitations include its inability to capture aesthetics and the potential for overlooking details in the window view (Li et al., 2022; Swietek and Zumwald, 2023).

2.2 Value of window views

Of all the studies that have explored the connection between window views and house

prices, water views have garnered the most attention (Bourassa et al., 2004). These studies have verified the positive impact on house prices of having a water view from a window, whether it is a river, lake, or bay (Luttik, 2000; Jim and Chen, 2009; Yamagata et al., 2016), barring a few instances of polluted water (Li et al. 2020). There are slightly fewer studies involving green views compared to water views, and most of them yield positive conclusions regarding green views (Jim and Chen, 2006; Wu et al., 2022). However, some argue that poor or excessive green views may also have negative impacts (Yamagata et al., 2016). Meanwhile, few studies have delved into the distinctions in the potential impacts of various types of green landscapes, such as trees and grasslands.

Sky and buildings are two of the most common landscapes in cities, however, they are rarely studied because they are difficult to quantify. To the best of our knowledge, only two hedonic studies have discussed sky views or building views. One of them, conducted by Swietek and Zumwald (2023), explores the interactive effects of sky and building views on cities through 3D city modeling. They observe that building views negatively impact house prices when the proportion of sky is low, but positively influence prices when the proportion of sky is high. Another study by Park et al. (2024), also employing 3D modeling, reveals a positive correlation between the proportion of sky and the price of house transactions. However, they also note that this correlation may be attributed solely to elevated floor levels. Additionally, several urban landscapes, such as roads, hard ground, barren ground, etc., have not been noticed by any research.

2.3 Computer vision methods relevant to this study

In recent years, advances in computer vision have facilitated the widespread application of semantic segmentation for quantitative studies of landscapes. From the early FCN (Long et al., 2015) and SegNet (Badrinarayanan et al., 2017) to recent models such as DeepLab (Chen et al., 2018) and SegFormer (Xie et al., 2021), full convolutional layers, self-attention, and other mechanisms have further improved the accuracy of semantic segmentation. These models have been used to quantify landscapes in various types of image data, such as street view imagery, remotely sensed imagery, unmanned aerial vehicle imagery, or self-taken photographs, enabling further analyses (Sun et al., 2022; Fan et al., 2023; Luo et al., 2022; Li et al., 2021; Ito and Biljecki, 2021).

The quantity of training data significantly influences the outcomes of deep learning algorithms (Xu et al., 2024). However, due to the constraints posed by the limited training dataset developed in this study, various data augmentation techniques are

essential for broadening the dataset. Data augmentation constitutes a pivotal phase within the deep learning model training process, generating supplementary training samples through the transformation and enhancement of the original dataset (Xu et al., 2024; Su et al., 2021). Additionally, addressing obstructions in images, such as railings in window views, is crucial for accurate segmentation. Image inpainting techniques based on deep learning have been widely applied to reconstruct missing or obscured parts of an image, enhancing the overall quality of the segmentation results (Quan et al., 2022).

3. Materials and methods

3.1 Window view data profile

The window view data required for the study was obtained from Lianjia (lianjia.com). In recent years, many real estate online platforms have introduced virtual tours (or 3D tours) to cater to the demand of homebuyers who wish to view properties remotely. These platforms offer panoramic photos of the interior, including balcony window pictures. As shown in Figure 1(a), when the server receives a client request for a virtual tour, it provides panoramic views from 6 images hosted on the server: up, down, left, right, front, and back, each with a resolution of 2048*2048 pixels. These images are combined to form a cubemap, which can then be projected as an equirectangular image. The server configures the 3D rendering pipeline based on parameters provided by the HTTP request to map the cubemap or equirectangular image to the cubemap model, providing users with a central, undistorted fisheye image similar to Figure 1(c). Users can zoom in and out using the mouse wheel. Figure 1(d) demonstrates this, showing an image generated from an isometric rectangular image with a smaller focal length and a higher distortion factor. The fisheye image in Figure 1(c), while achieving distortion-free in the central portion, exhibits significant distortions at the edges. In the equirectangular images, distortion is more pronounced in the top and bottom sections, whereas it is less pronounced in the middle portion containing the window view. Therefore, after thorough consideration, we opted to directly use the equirectangular image for segmentation, as this could be the optimal choice to reduce distortion-induced errors. In compliance with the website robots.txt protocol, we utilized a Python crawler program to locate all the house balconies required for our study and collected the cubemap provided by the balcony window view.

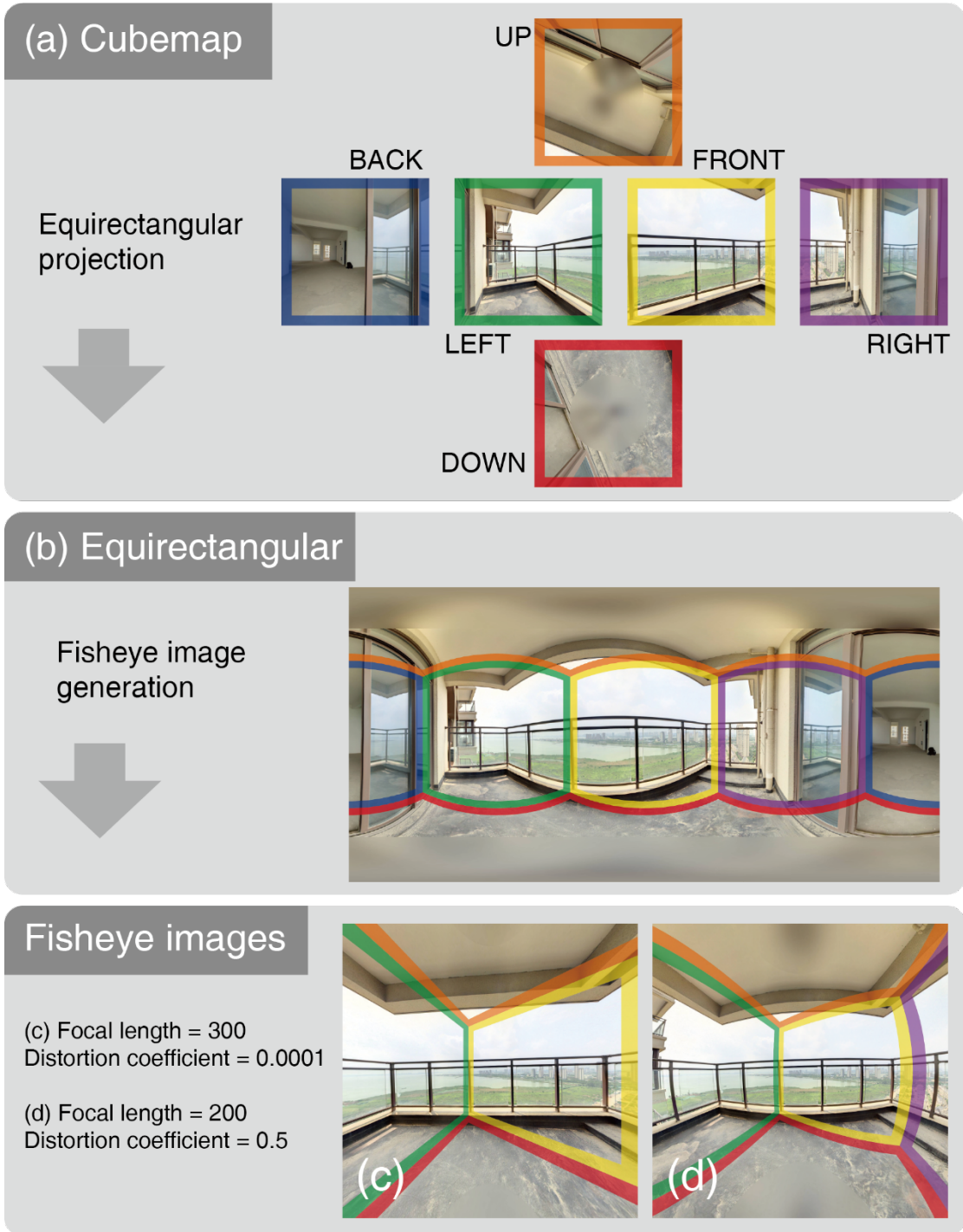


Fig.1. Example of images used in this research and their processing: (a) The cubemap of 6 images obtained from the website; (b) The equirectangular image obtained from the cubemap based on equirectangular projection; (c) The fisheye image is obtained from the equirectangular image using the Field of View camera model with a focal

length of 300 and a distortion coefficient of 0.0001; (d) The fisheye image has a focal length of 200 and a distortion coefficient of 0.5

3.2 Study area

China underwent significant housing system reform over a period of approximately six years from 1993 to 1998. This reform marked the discontinuation of the traditional welfare housing system and the introduction of a commercialized housing system. The photograph in Figure 2(c) illustrates a representative example of a Chinese urban community following commercialization. It features one or multiple high-rise apartment buildings, internal roadways, landscaped areas, and recreational spaces, all enclosed within a perimeter wall. Consequently, the factors influencing apartment prices in China can be categorized into two levels: inter-community differences and intra-community differences.

Wuhan, our study area, is a city located in central China and it is the core city of the Yangtze River Economic Belt. With rapid economic development in the past decades, the resident population of Wuhan has grown significantly, reaching 13.64 million by the end of 2021 (Wuhan Municipal Bureau of Statistics, 2022). This growth has resulted in a vibrant real estate market. The presence of numerous water bodies contributes to Wuhan's diverse landscape, but also limits available land for urban planning and construction, leading to high population density. With over 1,500 super-tall residential blocks, defined as those exceeding 30 stories, Wuhan ranks second in the country after Chongqing (Beike Research Institute, 2020). The abundance of supertall residential buildings and diverse landscapes in Wuhan offers a wide array of window views, making it an ideal choice for our study.

3.3 Data collection and processing

In August 2022, we collected sample data of apartments listed for sale in subdivisions, built in Wuhan within the last 5 years. We chose to limit the completion time to 5 years for several reasons. Firstly, the total number of apartments listed for sale in Wuhan on this platform exceeds 100,000, making it impractical to crawl through all of them. Additionally, manual screening at a later stage would be too time-consuming. Secondly, super-high-rise buildings constitute a relatively high proportion of those built in the last 5 years, providing a richer diversity of window views. Thirdly, most homebuyers choose to seal their balconies with glass during the apartment decoration process. The effect of glass shading may impact semantic segmentation accuracy in the later stage.

Houses whose balconies are not closed offer a higher quality data source.

The collected data include 6 cubemap shots taken at the balcony, the listing price of the apartment, the total number of floors in the building, the specific floor level (categorized as low, medium, and high floors), the property fee, and other apartment and community attributes (Figure 2) (Table A.1). We collected data from 9,722 apartments for sale in 598 communities built in Wuhan in the past five years, constituting the initial dataset.

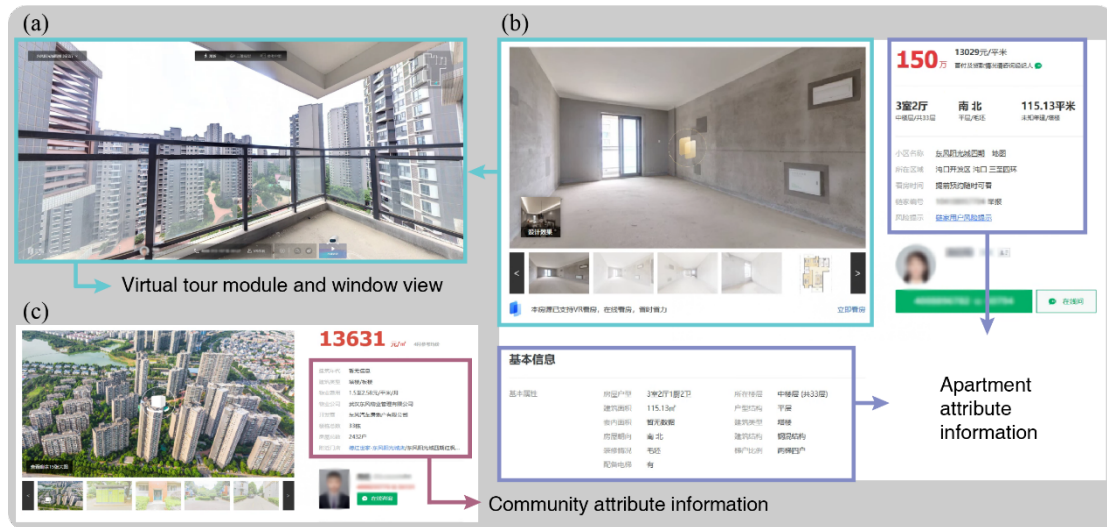


Fig.2. Relevant data of this study in the website: (a) virtual tour module, (b) apartment attribute webpage, (c) community attribute webpage.

As illustrated in Figure 3, we initially obtained 6 cubemap images with a resolution of 2048×2048 pixels for the living room balconies of 9722 apartments. These images were subsequently converted into equirectangular images with a resolution of 6400×3200 pixels. To ensure the quality of the semantic segmentation, we manually screened the photos to remove any low-quality images that could potentially affect the outcomes. Figure 3(a-e) highlights some of the common issues found in the excluded photos.

To address potential bias introduced by the removal of low-quality images, we conducted tests on the retained and removed samples across several variables. Our analysis revealed that the window views of undecorated samples generally performed better, making them more likely to be retained. This introduced some price differences between the two groups. However, for geographic variables, the Mann-Whitney U test

results for Longitude (p-value > 0.05) and Latitude (p-value > 0.02) indicate no significant difference in geographic distribution between the retained and removed data at the 1% significance level. The detailed methods and results of these analyses are provided in the Supplementary Material.

Following the screening process, we obtained 3041 usable apartment window view data points, forming the dataset for semantic segmentation. To facilitate subsequent manual annotation and accelerate deep learning training, we further reduced the image resolution, as outlined in Figure 3(3-4). Finally, Figure 3(5) illustrates the spatial distribution of the sample communities, which is crucial for understanding the geographic context of the retained data.

1. Convert cubmaps to equirectangular images



9722×6 pictures 2048×2048 pixel



9722 pictures 6400×3200 pixel



a. Overly oblique shooting angle



b. Closed balconies lead to indistinguishable window views



c. Heavy fog



d. Overexposed



e. Extensively obscured

2. Screen out unavailable images

3041 pictures 6400×3200 pixel

3. Crop the irrelevant edges part



3041 pictures 6400×2240 pixel



3041 pictures 4400×2240 pixel

4. Scale by 0.5 times for training



3041 pictures 2200×1120 pixel

5. Obtain research dataset

3041 apartment samples with window view images distributed in 452 communities

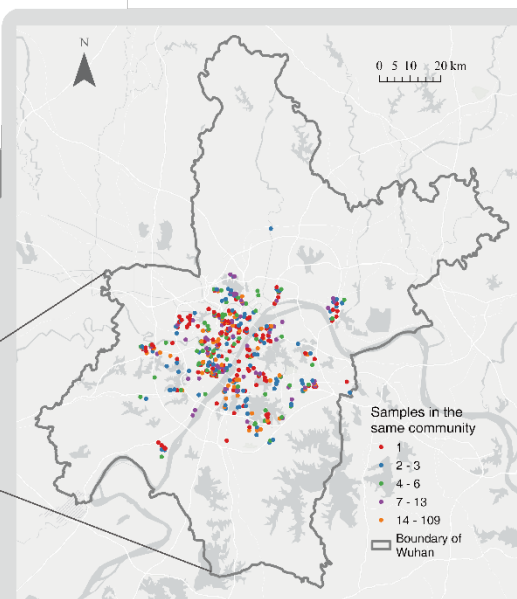
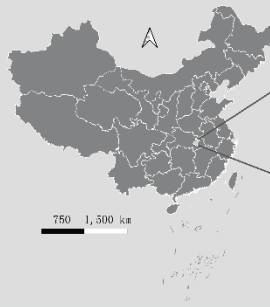


Fig.3. The processing flow of the window view dataset and the distribution of community samples. Source of the basemap: (c) ESRI.

3.4 Semantic segmentation of the window view dataset

The study conducted by Li et al. (2022) utilized transfer learning based on the Cityscapes dataset to semantically segment the simulated window views. However, transfer learning did not perform as expected in our dataset, likely due to the presence of both indoor and outdoor scenes in our real window views. While the sky and green space in most of the images can be effectively recognized, the weights based purely on outdoor environments in Cityscapes are insufficient for accurately identifying railings and indoor walls.

As a result, we chose to segment the window view dataset by manually labeling a portion of the data for training. We randomly selected 300 images from the dataset and performed pixel-level manual labeling using EISeg (Xian et al., 2016).

Li et al. (2022) categorized window views into four types: Green, Water, Sky, and Construction, while Hasegawa et al. (2022) further differentiated Construction into “Build” and “Traffic”. In our study, the landscapes in the window views were classified into 11 distinct categories, with each classification label and definition detailed in Table 1. Given the characteristics of window view samples in Wuhan, where high-rise buildings and trees can obstruct views, we further refined our categorization by subdividing “Buildings” into “High-rise buildings” and “Low-rise buildings”, and “Green” into “Trees” and “Grasses”.

Table 1. Classification labels and definitions

Labels	Definitions
Sky	Sky
High-rise buildings	Buildings with equal or more than 7 floors
Low-rise buildings	Buildings with less than to 7 floors
Grasses	Grasses
Hard ground	Hard ground, including roads within the community, sidewalks, parking lots and hard surfaces for recreation
Trees	Trees or shrubs
Water	Water landscapes outside the window such as rivers, lakes, etc.

Roads	Main avenue or railway outside the community
Barren land	Non-hardened barren land without any cover
Railings	Different styles of railings
Building interior	All landscapes of the interior of the apartment other than the window view, including the façade of this building in the window view

Note: The rationale for using 7 floors as the demarcation line between high and low buildings is based on the “Design code for residential building” in China (Ministry of Housing and Urban-Rural Development of the People's Republic of China, 2011). This code divides buildings into two categories based on whether they must be equipped with accessible elevators: buildings with less than seven floors, and buildings with seven or more floors.

Our approach encompassed a spectrum of data augmentation methodologies, including gamma transformation, random gamma transformation, rotation, blur, and noise addition. These augmentation strategies served to bolster the volume of our training dataset, consequently yielding notable enhancements in the accuracy of semantic segmentation. Through data augmentation, we obtained 1800 images available for training, of which 90% were classified as the training set and 10% as the validation set.

We chose SegNeXt as our semantic segmentation model (Guo et al., 2022). SegNeXt has redesigned convolutional attention and employs an efficient encoder-decoder semantic segmentation architecture, which achieved better results than DeepLab V3+ and SegFormer in both indoor ADE20K and outdoor Cityscapes datasets (Guo et al., 2022). We performed 120,000 iterations to obtain training weights using the segnext.large model and calculated Pixel Accuracy (Acc) and Intersection over Union (IoU) for all indices of elements after training and evaluated the overall accuracy of training using Mean Accuracy (mAcc) and Mean Intersection over Union (mIoU). After completing the learning to obtain the model weights, we semantically segmented all 3041 images and calculated the proportion of pixels occupied by different labels for each image.

3.5 Preparatory work before window view quantification

Before quantifying the window view, several issues need to be addressed. First, the angles at which the window view images were taken are not uniform, and it needs to be experimentally verified to what extent the shooting angle affects the presentation of the

window view. Second, equirectangular images exhibit significant distortion at the top and bottom, and it is necessary to ascertain whether this distortion affects the statistics of the window view. Finally, the styles of railings in different window view images vary, and the obstruction caused by railings may also lead to quantification errors. In this section, we need to verify or resolve the impact of these factors through various methods.

Our experiments demonstrate that the shooting angle and the distortion of the equirectangular images do not have a significant impact on the quantification of the window view. Due to space constraints, the details of these experiments are provided in the supplementary materials. The obstruction caused by railings essentially results in a loss of information, so we considered using generative artificial intelligence to address this issue. After semantic segmentation, we extracted the masks of the railings and used the DeepFill v2 model to inpaint the areas covered by the railings (Yu et al., 2019), as illustrated in Figure 4. However, although the initial inpainting made the railings thinner, it did not completely eliminate the railings. Therefore, we dilated the mask of the railings outward by 20 pixels and performed a second inpainting using the LaMa model (Suvorov et al., 2022).

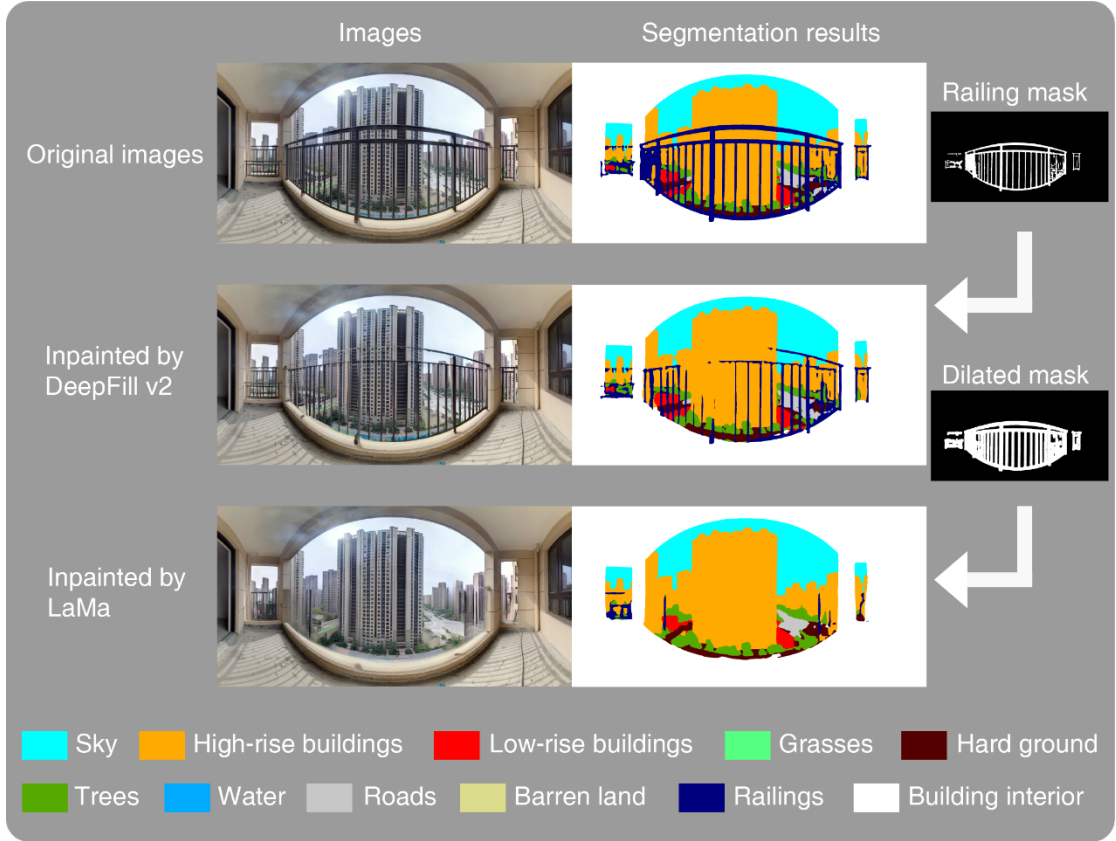


Fig.4. Inpainting process for the railings.

3.6 Calculation of window view indices

We quantified the composition of the sample window views using the Window View Index (WVI). For element i in the window view, its WVI_i can be calculated as follows (Li et al. 2022; Domjan et al. 2023; Bolte et al. 2024):

$$WVI_i = \frac{p_i}{1 - p_{buid_in} - p_{railing}} \quad (1)$$

Where p_i is the proportion of pixels of the element i after segmentation and inpainting. The types of elements i include Sky, High-rise buildings, Low-rise buildings, Grass, Hard ground, Trees, Water, Roads, and Barren land. p_{buid_in} is the

proportion of pixels segmented as Building interior, and $p_{railing}$ is the proportion of pixels segmented as Railing.

3.7 Spatial hedonic price model

3.7.1 Variable selections

We choose the variables in Table 2 to form the hedonic price model based on two considerations. Initially, to address endogeneity concerns, we incorporated all potential factors that might influence the variables related to the WVI into the model. For instance, the window size could vary depending on factors such as the building's construction year and apartment area. Similarly, the landscape outside the window could be intricately linked to the floor level and geographical location of the apartment. Secondly, factors such as school districts and subway proximity significantly influence housing prices in China (Wen et al., 2017; Duan et al., 2021). Therefore, based on previous research on hedonic price analysis in Wuhan, we collected a total of 511 points of interest (POIs) and areas of interest (AOIs) data closely related to housing prices (Liu et al., 2020).

The area, age, floor, total floor, decoration situation, elevator-to-apartment ratio, and property fee were obtained from lianjia.com. Distance variables and shop convenience variables were calculated in ArcGIS Pro using POI data obtained from Baidu.com and AOI data obtained from OpenStreetMap. Additionally, WVI variables were calculated using the formula described in section 3.6.

Table 2. Variables, definitions and descriptive statistics.

Variables	Definitions	Min	Mean	Max
Dependent variable				
Price	Price per m ² of the apartment (CNY /m ²)	4005	17,697.68	79,639
Structural variables				
Area	Total area of the apartment (m ²)	21.57	112.95	378.67
Age	Year of the building construction (year)	0	4.67	5

Floor	The apartments are on the low, middle and high floors of the building, assigned as 1 (n=1113), 2 (n=1102) and 3 (n=826) respectively	-	-	-
Tot_floor	Total floors of the building where the apartment is located	3	33.08	58
Decoration	Dummy variables for apartment decoration state: decorated for 1 (n=1176); undecorated for 0 (n=1865)	-	-	-
E2A_ratio	Elevator-to-apartment ratio: The ratio of the elevator number in the building where the apartment is located to the number of apartments on each floor	0.14	0.56	2.00
Prop_fee	Property fees for the community where the apartment is located (CNY/m ² /month)	0.55	2.85	7.80
Neighborhood variables				
Dis_pri	Euclidean distance between the apartment and the nearest key primary school (m)	208.45	8051.94	32,365.19
Dis_mid	Euclidean distance between the apartment and the nearest key middle school (m)	223.06	4036.13	19,747.24
Dis_uni	Euclidean distance between the apartment and the nearest university (m)	14.13	720.78	4569.81
Dis_hos	Euclidean distance between the apartment and the nearest 3A hospital (m)	205.03	3754.69	18,336.22
Dis_sub	Euclidean distance of the apartment from the nearest subway station (m)	44.39	1091.94	6576.49
Dis_aero	Euclidean distance between the apartment and Wuhan Tianhe Airport (m)	2895.50	20,874.39	34,940.16

Dis_train	Euclidean distance of the apartment from the nearest train station (m)	512.69	9920.50	34,798.96
Dis_rail	Euclidean distance of the apartment from the nearest railroad (m)	40.88	2467.32	21,221.68
Dis_road	Euclidean distance of the apartment from the nearest highways and overpass (m)	14.13	774.86	4569.81
WVI variables				
WVIsky	Window view index of sky	0.00	0.35	0.81
WVIhigh	Window view index of high-rise buildings	0.00	0.39	0.94
WVIlow	Window view index of low-rise buildings	0.00	0.05	0.46
WVIgrass	Window view index of grasses	0.00	0.02	0.46
WVIhard	Window view index of hard ground	0.00	0.04	0.34
WVItree	Window view index of trees	0.00	0.14	0.96
WVIwater	Window view index of water	0.00	0.00	0.28
WVIroad	Window view index of roads	0.00	0.01	0.19
WVIbarren	Window view index of barren land	0.00	0.01	0.34

3.7.2 Model strategy and diagnostic

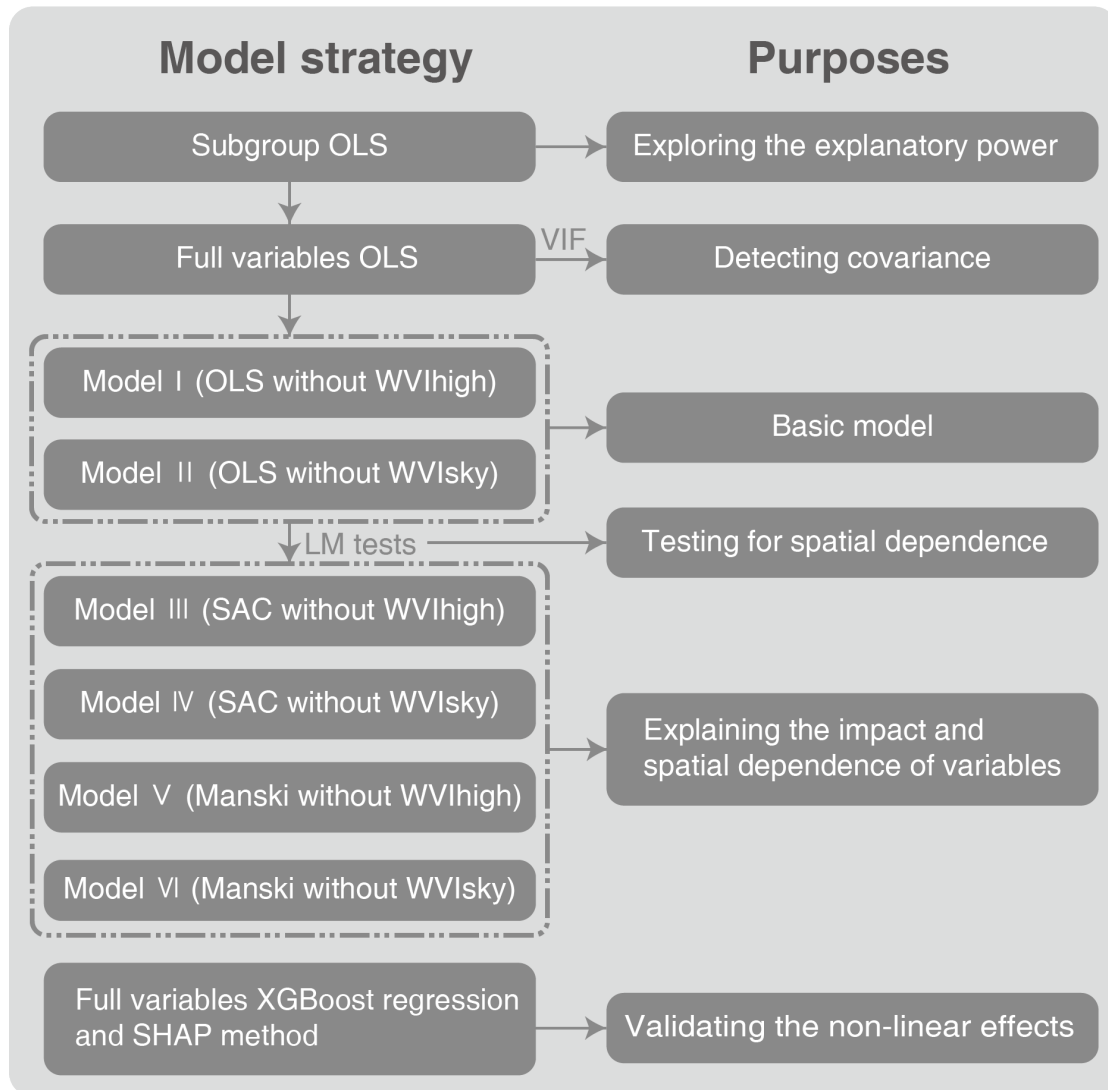


Fig. 5. Modelling strategy and purposes (OLS: Ordinary Least Square, VIF: Variance Inflation Factors, SAC: Spatial Autoregressive Confused)

The strategy of our hedonic price model is shown in Figure 5. First, we separate OLS models based on structural, neighborhood, and WVI variables, which are used to compare the explanatory power of each set of variables for house prices. Considering the long-tailed distribution of house price variables and neighborhood variables, we logarithmically transform these two types of variables to reduce the heteroscedasticity in the models. The formulas for the grouped models are as follows:

$$\ln(\text{Price}) = \alpha_1 + \beta_1 \text{Stru} + \varepsilon_1 \quad (2)$$

$$\ln(\text{Price}) = \alpha_2 + \beta_2 \ln(\text{Neig}) + \varepsilon_2 \quad (3)$$

$$\ln(\text{Price}) = \alpha_3 + \beta_3 \text{WVI} + \varepsilon_3 \quad (4)$$

Where $\ln(\text{Price})$ donates the log of apartment price, α_1 , α_2 , α_3 are the constants, Stru , $\ln(\text{Neig})$, WVI represent the structural variables, the log of neighborhood variables, WVI variables respectively. β_1 , β_2 , β_3 are the coefficients to be estimated, ε_1 , ε_2 , ε_3 are the error terms.

Subsequently, we constructed full-variable Ordinary Least Squares (OLS) models and assessed their Variance Inflation Factors (VIF), which revealed the existence of multicollinearity issues within the model (Table A.2). Therefore, we first deleted the variable Dis_uni and Dis_road , followed by removing the variables WVIhigh and WVIsky from two different models, named as Model I and Model II, respectively:

$$\ln(\text{Price}) = \alpha + \beta_1 \text{Stru} + \beta_2 \ln(\text{Neig}) + \beta_3 \text{WVI} + \varepsilon \quad (5)$$

3.7.3 Spatial regression model

Another pertinent issue necessitating our attention involves spatial dependence. The house prices and window views, along with other features that are factored into the error term, exhibit a close association with the geographic location of the apartment. Disregarding spatial dependence and non-stationary effects within the model could result in biased estimations of coefficients when employing OLS, thereby potentially reporting spurious significance (Qiu et al., 2022). In this case, spatial regression models that can eliminate the influence of spatial relationships would be a better choice.

As the most complete spatial interaction model, the Manski model covers three spatial interactions, including a lagged dependent term (WY), an autocorrelated error term ($W\mu$), and exogenous spatial interaction terms (WX), which can be represented as (Manski, 1993):

$$\begin{aligned} Y &= \rho WY + \alpha i_N + X\beta + WX\theta + \mu \\ \mu &= \lambda W\mu + \varepsilon \end{aligned} \quad (6)$$

Where Y is the vector of apartment prices (which is $\ln(\text{Price})$ in this study), ρ is

the spatial autoregressive parameter (spatial lag), W is the spatial weight matrix, X is the matrix of exogenous explanatory variables, β is the matrix of parameter coefficients associated with explanatory variables, θ is the matrix of parameter coefficients for lagged explanatory variables, μ is the vector of spatially correlated disturbance terms, λ is the spatial autocorrelation (error) parameter, and ε is the vector of independently and identically distributed error terms. When $\theta = 0$, Manski can degenerate into a spatial autoregressive confused (SAC) model:

$$\begin{aligned} Y &= \rho WY + \alpha i_N + X\beta + \mu \\ \mu &= \lambda W\mu + \varepsilon \end{aligned} \quad (7)$$

We constructed the distance spatial weight matrix on the assumption that each sample has at least one neighbor. Lagrange multiplier (LM) tests are used to detect the spatial dependence of the dependent variable and the error term in OLS models (Anselin, 1988). The outcomes of LM tests indicated the presence of spatial dependence within both the dependent variable and the error term in the OLS model (Table A.3). Specifically, neither ρ nor $\lambda \neq 0$, indicating that the SAC model cannot further degenerate.

Therefore, the SAC and Manski forms of Model I and Model II are named as Model III, IV, V, and VI, respectively, to further elucidate the impact of the WVI variables on apartment prices. The coefficients are estimated by the "sacsarlm" function based on the maximum likelihood estimation in the "spatialreg" package of R (Bivand et al., 2021).

3.7.4 XGBoost and SHapley Additive explanation method

Given the potential for a non-linear relationship between WVI and apartment prices, which spatial hedonic price models may not capture., we integrated the XGBoost regression with the SHapley Additive explanation (SHAP) method to model the unaccounted nonlinear relationship within Equation (5). The SHAP method is based on the Shapley value theory of cooperative games in game theory. It allows for the application of the Shapley value to the contribution of features, thereby calculating the contribution of each feature to the prediction result (Lundberg and Lee, 2017; Sun et al., 2022). This non-parametric approach enhances our understanding of the intricate relationship between WVI and apartment prices by providing insights into the contribution of each feature to the prediction result.

4 Results

4.1 Semantic segmentation and image inpainting results

Figures 6(a) and 6(b) present the mAcc and mIoU for both the original and augmented data, as well as the Acc and IoU for each label. The results demonstrate that data augmentation has effectively enhanced the accuracy of semantic segmentation, particularly for labels that had poor classification performance in the raw data, such as low-rise buildings, hard ground, roads, and barrier land. Specifically, the mAcc improved from 68.72% to 86.33%, while the mIoU increased from 59.17% to 78.71%. Compared to other analytical papers involving semantic segmentation (Luo et al., 2022; Wang et al., 2021), this level of accuracy is sufficient for further analysis.

Figure 6(c) shows the proportion of each label after semantic segmentation of the images without inpainting, the proportion after inpainting, and the percentage change in the average values for each label. It can be observed that, in addition to railings and indoor parts, the sky, high-rise buildings, and trees are the most common landscapes in the window view of high-rise residential apartments in Wuhan. Low-rise buildings, grasses, hard ground, and roads are next in prevalence. As a "city of thousands of lakes", although the water area of Wuhan accounts for 25.73% of the total urban area, water landscapes are not widely visible in residential window views, with only 16.80% of views containing water bodies.

Examining the rate of change in the average values of each label before and after inpainting, the proportion of railings decreased by 96.67% after image inpainting. Significant increases were observed predominantly in ground-level landscapes that are easily obstructed by railings, including barren land (69.58%), water (40.04%), and tree (35.63%). Conversely, the proportion of sky, primarily situated in the upper part of the window view and less obstructed by railings, exhibited a modest increase of 5.49%. These results confirm that image inpainting effectively reduces railing obstructions and appropriately restores landscapes obstructed by railings.

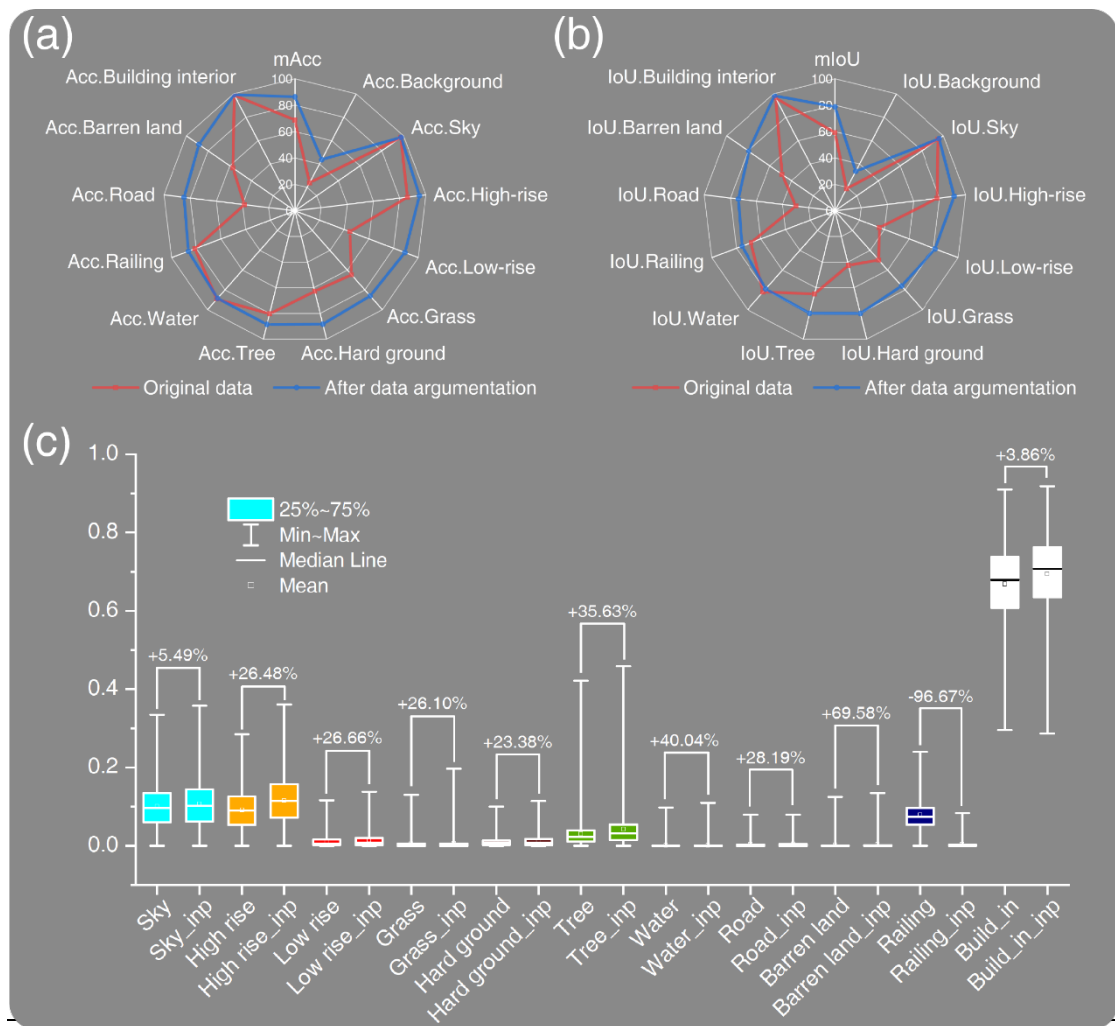


Fig.6. Semantic segmentation and image inpainting results: (a) mAcc and Acc of each label in original data and data after augmentation, (b) mIoU and IoU of each label in original data and data after augmentation, (c) the proportion of each label after semantic segmentation of the images without inpainting, the proportion after inpainting, and the rate of change in the average values for each label.

4.2 Results of OLS

Table 3 presents the outcomes detailing the explanation of apartment prices by structural variables, neighborhood variables, and WVI variables, respectively. All variable groupings pass the F-statistic test ($p < 0.01$), suggesting their collective capacity to elucidate apartment prices as distinct variable groups. However, substantial discrepancies exist in their respective levels of explanatory power. Specifically,

neighborhood variables can explain 64.3% of the variance in apartment prices, followed by structural variables at 38.8%, while WVI variables lag significantly with an explanatory power of 2.3%.

Table 3. OLS modeling with different variable groups.

	Structural variables	Neighborhood variables	WVI variables
No. of variables	7	9	9
Adjusted R ²	0.388***	0.643***	0.023***
S.E. of regression	0.334	0.255	0.422

***significant at $p < 0.01$.

Table 4 displays the outcomes of the OLS Model I and II. The coefficient estimations for structural and neighborhood variables align closely with findings from the previous study of Wuhan (Peng et al., 2023). Factors such as area, floor, decoration, elevator-to-apartment ratio, and property fees have a positive impact on selling prices. Key primary schools, hospitals, metro stations, and train stations positively influence nearby apartment values, while airports and railroads exert negative effects. However, we do not interpret the WVI variable further due to potential spatial dependence issues within the OLS model.

Table 4. Estimated coefficients of OLS models.

Models	Model I	Model II
Constant	10.907***	10.908***
<i>Structural variables</i>		
Area	0.001***	0.001***
Age	0.002	0.002
Floor	0.013*	0.013*
Tot_floor	-0.003***	-0.003***

Decoration	0.026***	0.026***
E2A_ratio	0.067**	0.067**
Prop_fee	0.144***	0.144***
<i>Neighborhood variables</i>		
ln(Dis_pri)	-0.249***	-0.249***
ln(Dis_mid)	-0.006	-0.006
ln(Dis_hos)	-0.015**	-0.015**
ln(Dis_sub)	-0.042***	-0.042***
ln(Dis_aero)	0.136***	0.136***
ln(Dis_train)	-0.076***	-0.076***
ln(Dis_rail)	0.026***	0.026***
<i>WVI variables</i>		
WVIsky	-0.002	—
WVIhigh	—	-0.002
WVIlow	-0.072	-0.073
WVIgrass	-0.362***	-0.363***
WVIhard	-0.118	-0.120
WVItree	0.039	0.038
WVIwater	0.298	0.297
WVIroad	-0.048	-0.047
WVIbarren	-0.494***	-0.495***
Adjusted R ²	0.725	0.725
AIC	-439.233	-439.233

*Significant at $p < 0.1$; ** Significant at $p < 0.05$; ***significant at $p < 0.01$.

4.3 Results of spatial regression models

Table 5 summarizes the coefficient estimates of the SAC model and Manski model. In this section, our focus lies primarily on the impact of WVI variables, so the coefficient estimates for structural variables and neighborhood variables are omitted. The spatial error terms (λ) are significant in all spatial models, while spatial autoregressive terms (ρ) are only significant in the SAC model. This suggests that in Manski models, the lagged explanatory variables $WX\theta$ serve as substitutes for the explanatory power of the spatial autoregressive term ρWY . The significance revealed by the likelihood ratio (LR) test implies that none of the four spatial models could be reduced.

Regarding goodness of fit, two Manski models outperform the SAC models, as

indicated by an increase in the Nagelkerke Pseudo R^2 from 0.861 to 0.874 and the reduction in the Akaike Information Criterion (AIC) from -2499.3 to -2735.7. Therefore, the following discussion will focus primarily on the results of the two Manski models. Additionally, it should be noted that in Manski models, the coefficient of individual spatial interaction term $W * WVI_i$ is closely related to the configuration of the spatial weight matrix W . Thus, we focus solely on determining the direction (positive or negative) of its influence, rather than delving into detailed interpretations of the coefficient values.

Table 5. Estimated coefficients of spatial models.

Models	Model III SAC	Model IV SAC	Model V Manski	Model VI Manski
Constant	6.315***	6.274***	18.067***	15.722***
Structural variables	YES	YES	YES	YES
Neighborhood variables	YES	YES	YES	YES
WVIsky	-0.024		-0.028	
WVIhigh		0.024		0.028
WVIlow	-0.128**	-0.104	-0.068	0.041
WVIgrass	-0.269***	-0.245***	-0.327***	-0.300***
WVIhard	-0.169**	-0.145*	-0.166**	-0.138*
WVItree	-0.025	-0.002	-0.040	-0.012
WVIwater	0.987***	1.010***	0.782***	0.810***
WVIroad	0.215*	0.39*	0.124	0.151
WVIbarren	-0.184*	-0.161	-0.151	-0.124
$W*WVIsky$	–	–	-0.748	
$W*WVIhigh$	–	–		0.749
$W*WVIlow$	–	–	1.518	2.267
$W*WVIgrass$	–	–	-8.590***	-7.842***
$W*WVIhard$	–	–	0.355	1.104
$W*WVItree$	–	–	-0.278	0.470
$W*WVIwater$	–	–	-9.134*	-8.385*
$W*WVIroad$	–	–	-14.444***	-13.694***
$W*WVIbarren$	–	–	3.716	1.584
ρ	0.391***	0.391***	-0.261	-0.261

λ	0.941***	0.941***	0.986***	0.986***
LR test value:	2064.1***	2064.1***	2344.5***	2344.5***
Pseudo R ²	0.861	0.861	0.874	0.874
AIC	-2499.3	-2499.3	-2735.7	-2735.7

*Significant at $p < 0.1$; ** Significant at $p < 0.05$; ***significant at $p < 0.01$.

4.4 XGboost and SHAP results

The outcomes from our application of the XGBoost regression and the SHAP method to Equation (5) are illustrated in Figure (7). The XGBoost regression yielded an R² of 0.948 and an RMSE of 0.098, indicating that our model achieved a good fit in XGBoost regression. Similar to the results obtained from the OLS models, the structural variables and the neighborhood variables manifest a greater impact on apartment prices, whereas the window view variable exhibits comparatively lesser importance. Elevated values associated with schools, metro, and hospitals correspond to lower SHAP values, indicating that apartments situated farther from these amenities tend to have lower prices. Conversely, being situated at a greater distance from the airport is viewed as a positive factor. Furthermore, the influences of property fees, total area, and renovation align closely with the findings from the OLS models. This consistent alignment underscores the reliability and robustness of machine learning and SHAP methods in understanding the factors influencing apartment prices, similar to traditional regression methodologies.

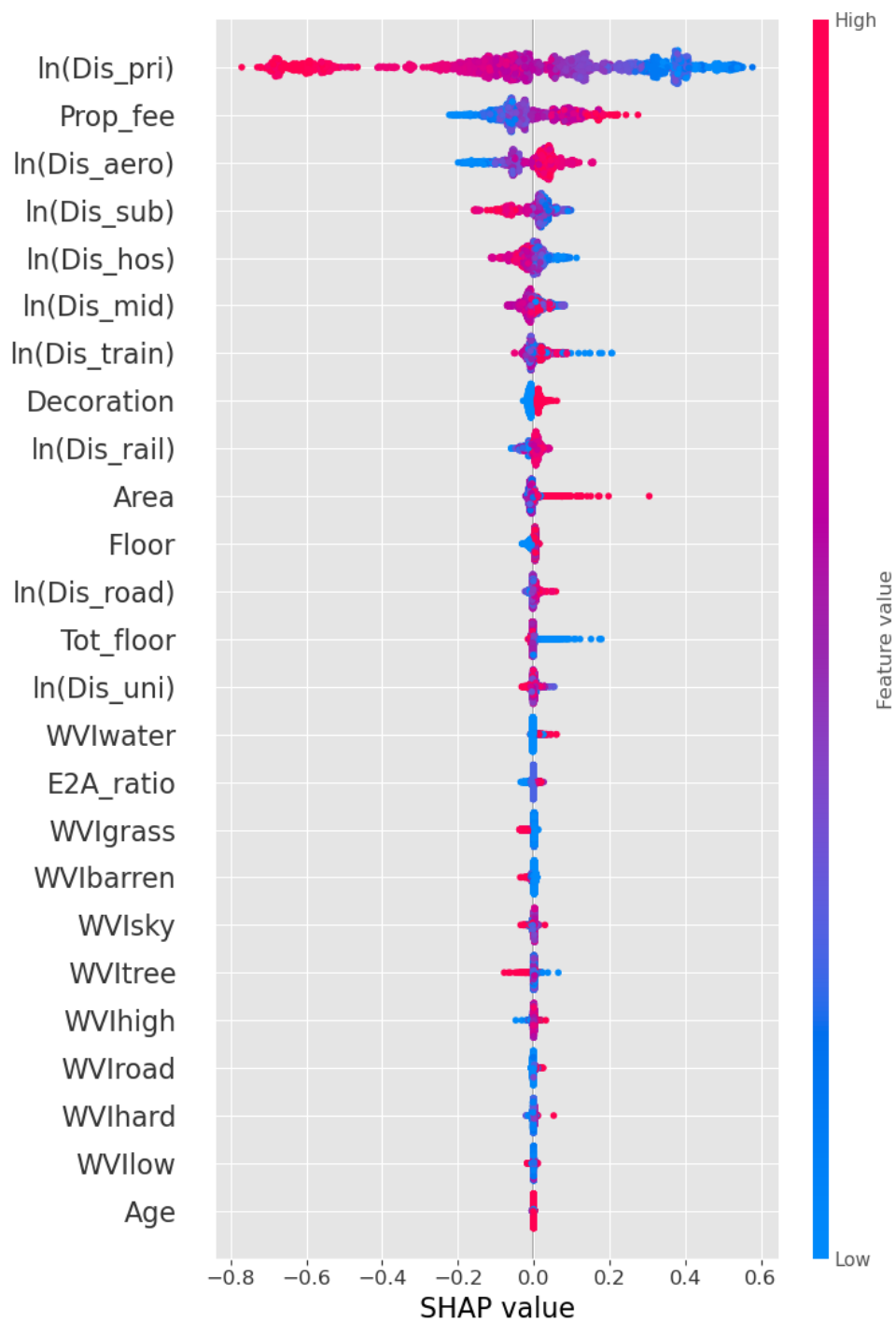


Fig.7. Result of XGBoost and SHAP method

Figure 8 presents scatter plots of the nine WVI variables against their SHAP values, with a LOWESS regression curve fitted to the data. In summary, Moderate values of

WVisky are associated with higher SHAP values, while extremely low or high values correspond to decreased SHAP values. Notably, SHAP values tend to exhibit predominantly positive trends for WVIgrass below 0.05, while values above 0.05 tend to display negative trends, where WVIhard does not exhibit a discernible trend. Additionally, SHAP values for WVIwater demonstrate a linearly positive correlation with this variable.

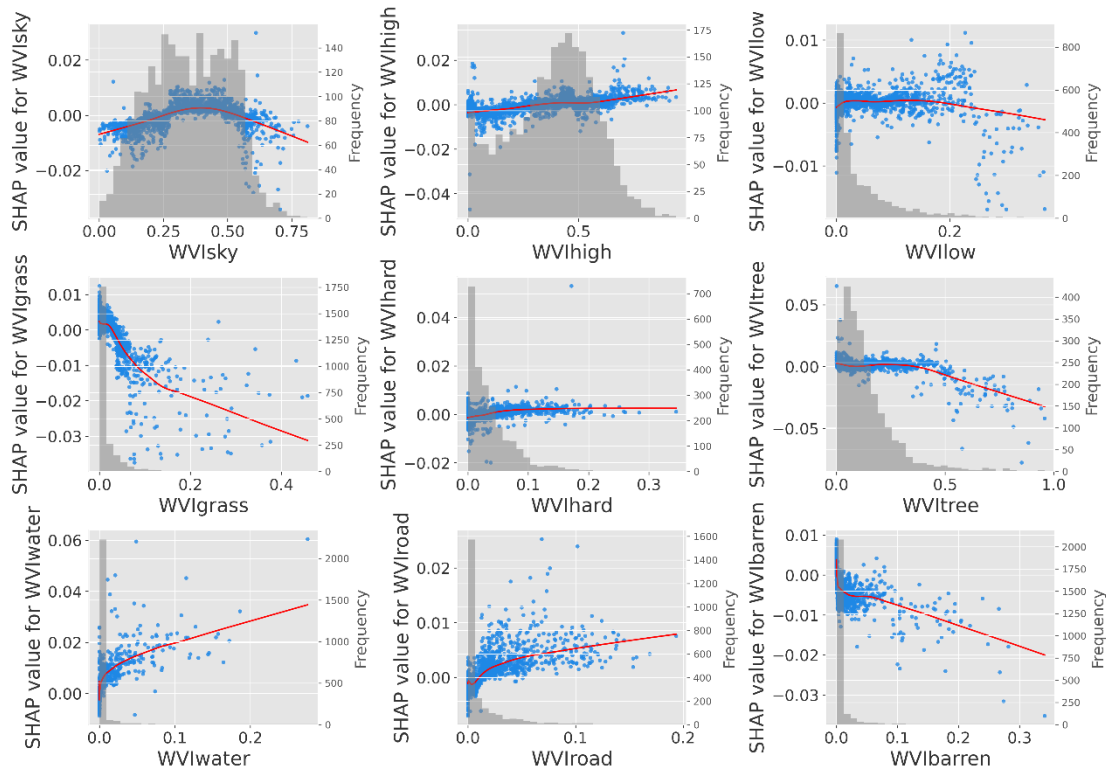


Fig.8. Scatter plot of SHAP values for window view variables

5 Discussion

5.1 Applicability of window view data

In this study, we developed a window view dataset from the virtual tour module of a real estate online platform, which provides a new and available data source for window view and cityscape-related studies at a large scale. We also checked some real estate online platforms in other countries and found that such data exists on a large scale (Figure 9a, 9b), affirming the potential for extending our dataset to encompass cross-city and even cross-country scales.

The approach can potentially offer benefits for studies involving window views and cityscapes. As shown in Figure 9, aside from the reflection on the glass and the bokeh sky in Figure 9(d), our training weights performed well in segmenting the window view. We suggest that when applying our training weights to other window view datasets, cropping the images to reduce noise unrelated to the window view can enhance segmentation performance. This noise reduction technique can be particularly effective when applying our training weights to datasets from different regions.

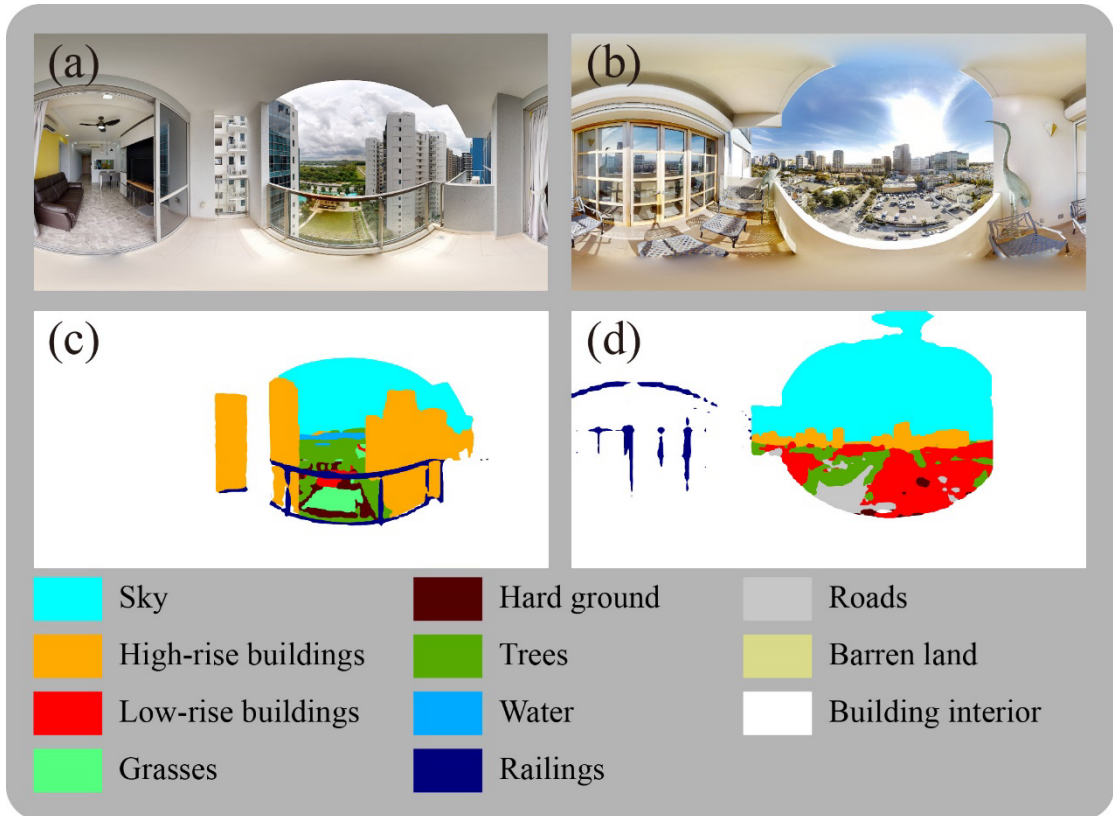


Fig. 9 Results of window view data from other countries and semantic segmentation using the weights from the experiments: (a) window view image of Singapore from <https://buycondo.sg/>; (b) window view image of Los Angeles, USA from <https://www.zillow.com/>; (c) semantic segmentation result of image (a); (d) semantic segmentation result of image (b).

Previous methods for quantifying window views, such as the dummy variable method, GIS-based viewshed analysis, or virtual window views generated from 3D CIM, have relied on virtualization to quantify window views, which entails inherent limitations. These shortcomings include challenges in accurately simulating the real shapes and

sizes of windows (Yamagata et al., 2016), difficulties in capturing the aesthetic qualities of specific views (Li et al., 2022; Swietek and Zumwald, 2023), potential oversights in minor yet significant landscapes such as neighborhood trees (Sander and Polasky, 2009), and the inability to capture internal views, which are important for how people perceive a space (Turan et al., 2021). In contrast, our approach utilizes real window views, partially overcoming the limitations of previous virtualization methods. It covers a wide spatial scale and provides easy accessibility, a substantial volume of data, and authentic photography. This method effectively captures the cityscape as viewed through residential windows, providing a more realistic representation compared to previous virtual methods.

Despite the potential advantages of our method, we also recognize some limitations. Similar to other still photographs, this data does not capture dynamic elements outside the window, such as puffy clouds, leaves swaying in the wind, moving vehicles, and crowd activity (Lin et al., 2022). Therefore, for future research endeavors, the integration of various methods is anticipated to enhance both the accuracy and comprehensiveness of window view analysis (Turan et al., 2021). Additionally, exploring dynamic elements using technologies like virtual reality (VR) may provide new perspectives and deeper insights into window view research (Ko et al., 2023; Van Renterghem et al., 2023). We are optimistic that this amalgamation of diverse methodologies will usher in new perspectives and deeper insights into the field of window view research.

5.2 The value of the window view elements

Another focus of our study is to assess the value of window views, specifically by investigating the significant impact of different types of window view elements on apartment prices in Wuhan using hedonic price models. In the following sections, we delve into the categorization of the landscapes considered in this study.

5.2.1 Sky and Buildings

Due to the multicollinearity arising from the highly negative correlation between WVI_{sky} and WVI_{high} , we estimated their coefficients in separate groups of models. Although the coefficients of WVI_{sky} and WVI_{high} were consistently opposite in direction across all groups, none of the models demonstrated statistical significance for either variable. These findings suggest the proportion of sky or high-rise buildings in the window view does not exert a significant linear effect on house prices.

However, the SHAP method brings some insights that the regression method failed to uncover. The effect of the sky is not linear but shows an inverted U-shape. Limited sky views might signify obstructed vistas and diminished daylight, while an excessive sky view could indicate isolated locations with scant commercial amenities. A more moderate view of the sky is preferable (Yao et al., 2024). In other studies, the sky elements also presented ambiguous characteristics. Some studies argue that the sky is the most popular landscape viewed from windows, and dynamic features such as clouds and birds in the sky promote attention recovery (Ko et al., 2022; Orquin and Loose, 2013). However, in some street view studies, the sky has been found to have a negative impact on perceptions, as a large exposure to the sky on the street can create a sense of insecurity (Rossetti et al., 2019; Xu et al., 2022).

WVIhigh and WVIlow are not significant in the Manski model, and in the SHAP results, they only exhibit a relatively weak trend. As buildings are the most common landscape in urban areas, the impact they cause may require further detailed research. Some studies on the subjective perception of window views have found that in high-density urban environments, views obstructed by tall buildings can make people feel oppressed (Chung et al. 2022). However, other research has found that 27% of participants prefer to see buildings from their window views (Lin et al. 2022). Additionally, the presence of distinctive structures like landmarks, skyscrapers, and buildings of historical or cultural significance can positively impact people's assessment of window views (Damigos and Anyfantis, 2011).

5.2.2 Natural landscapes

In all regression models, WVItree did not exhibit a significant influence on apartment prices in Wuhan. Considering the low SHAP values associated with high WVItree indices (exceeding 0.4) as per the SHAP methodology, it can be inferred that a limited number of trees visible from the window exert an insignificant impact on house prices, while an excessive tree presence might even yield a negative effect. A moderate quantity of trees in the window view is perceived favorably, whereas a dense tree cover may suggest lower apartment floors and reduced natural light, potentially evoking feelings of isolation or seclusion (Cao and Huang, 2023).

In all regression models, WVIgrass was found to exert a significant negative impact on apartment prices in Wuhan. In the two Manski models, for every 1% increase in WVIgrass, apartment prices decrease by 0.327% and 0.300%, respectively. Moreover, the spatial interaction term $W*WVIgrass$ in Manski models also exhibited a significant

negative coefficient. Correspondingly, the SHAP values for WVIgrass showed a rapid decline as WVIgrass increased. These findings collectively suggest that both the presence of grasses in the immediate window view and the broader vicinity are perceived negatively in the real estate market of Wuhan. This conclusion aligns with the observations made by Liu et al. (2020) in their Wuhan study, where they argue that an overabundance of grassland may impede the development of other types of land, thereby diminishing residents' convenience. Furthermore, few public grass landscapes exist in the urban area of Wuhan. Most of the grass observed in window views manifests as the paving of green landscapes within neighborhoods. This phenomenon might lead to higher visibility of grass predominantly in only window views from lower floors.

In Manski models, WVIwater is consistently identified as a positive factor, with a 1% increase in WVIwater leading to a 0.782% and 0.810% enhancement in apartment value. This positive impact is further validated by the linear increase in the SHAP value of WVIwater with its augmentation. Intriguingly, the endogenous spatial interaction term $W^*WVIwater$ in Manski's model exhibits a significant negative effect on property value. These findings suggest that while direct visibility of a water landscape from an apartment window commands a significant premium, its presence in the view of nearby samples may detract from the property's value. This could indicate that the attractiveness of blue spaces is more dependent on direct visibility rather than mere proximity. The value of visible water features is echoed in various studies: Damigos and Anyfantis (2011) highlight the high valuation of ocean views by real estate experts, and Hasegawa et al. (2022) argue the positive impact of window water features in mitigating the psychological distress associated with otherwise unappealing views. Conversely, for apartments without direct water views but situated nearby, potential drawbacks include mosquito breeding (Irwin et al., 2008), flood risks, and contamination concerns (Tang et al., 2020; Li et al., 2020), suggesting that proximity to water might not always be advantageous.

5.2.3 Other landscapes

In the spatial models, WVIhard has a negative impact. Specifically, a 1% increase in WVIhard leads to a 0.166% and 0.138% reduction in apartment prices. The lack of sensory appeal associated with hard surfaces may indicate a scarcity of green spaces in the vicinity, potentially diminishing the area's attractiveness.

WVIroad demonstrates a significant negative impact in the SAC model, yet this effect is not mirrored in the Manski model. Interestingly, the spatial interaction term

W^*WVI_{road} shows a significant positive influence. The visibility of a road from an apartment might suggest undesirable traffic noise (Chung et al., 2019), whereas its presence in a neighboring view may be interpreted as enhanced accessibility (Seo et al., 2014). Therefore, proximity to roads is valued more due to enhanced accessibility, whereas visibility of roads from apartments may be perceived as less beneficial or even detrimental, possibly due to concerns about traffic noise.

WVI_{barren} did not prove significant in any spatial models, so as its spatial interaction term, W^*WVI_{barren} . The SHAP method indicated an overall negative impact of WVI_{barren} . Predominantly, barren land in Wuhan represents undeveloped areas. Its visibility from an apartment might carry negative connotations, but a high concentration of such land in the surrounding area could suggest that the region is undergoing rapid development, potentially leading to higher future property values (Wen and Tao, 2015).

6 Conclusion

Our study employed computer vision to quantify the window views of residential apartments in Wuhan using data from real estate websites, and examined the impact of different window view elements on house prices through a spatial hedonic price model and an explainable machine learning approach. This analysis yielded several key findings. The results of semantic segmentation highlighted the effectiveness of data augmentation in improving accuracy for small datasets. In Wuhan, the most common landscapes visible from apartment windows were the sky and high-rise buildings, while water views were relatively rare. Moreover, the hedonic pricing model revealed that water views positively influence apartment prices, whereas views of grass and hard ground tend to have a negative impact on property values.

The main contributions of our study are as follows. Firstly, we developed a previously unexplored urban-scale window view dataset, providing a valuable new data source for researchers studying window views and their implications. In essence, we also introduced a new application for images scraped from real estate platforms. Secondly, while most previous studies on window views use various methodologies to simulate and reconstruct authentic window views, our study stands out by accurately calculating the composition of window views through real window view photos using computer vision and WVI. This approach not only enhances the accuracy of our analysis but also facilitates a deeper understanding of the association between each WVI and house prices. Finally, we made the semantic dataset used in the study openly available under the permissive Creative Commons Attribution 4.0 International license (CC BY 4.0) on

[Github](#) to support subsequent related studies.

However, our study is not without limitations. Our sample was limited to high-rise community residences built within the past five years. This selection may not fully reflect the diversity of window view characteristics found throughout the city, especially in older low-rise buildings. Additionally, while we primarily focused on the window views from living rooms, this approach does not account for the potential impact of views from other rooms, such as bedrooms, which could also influence house prices. Furthermore, the influence of waterscapes on house prices, as observed in Wuhan—a city known for its abundant water resources—may not be generalizable to cities with water scarcity. Future research could address these limitations by conducting comparative studies across multiple cities to further validate and expand upon these findings.

Our findings can be extended to the fields of urban planning, architectural design, and property development. For example, in Wuhan, water is still a scarce landscape, valued more for its visibility than proximity. Therefore, for waterfront areas, stepped-height building designs may be preferable to a large number of high-rise buildings. These designs optimize views, avoid overshadowing, and ensure that more households can enjoy the water view (Xue et al., 2022). For real estate developers, buildings in the waterfront area should be staggered, with a reasonably planned layout and spacing of high-rise buildings, allowing more households to enjoy the high-quality landscape. Additionally, developers can enhance the overall environmental quality of the neighborhood by incorporating trees and diverse greening elements. This not only reduces the negative impact of grass and hard landscaping but also effectively increases property sales prices.

Appendix

Table A.1. Summary of apartment and community attributes

Attribute Type	Item	Range/Types	Unit
Apartment Attributes	Price	200,000 to 24,600,000	CNY
	Price per m ²	4,005 to 79,639	CNY
	Bedrooms	0 to 6	units
	Living Rooms	0 to 4	units
	Kitchens	0 to 2	units
	Bathrooms	0 to 5	units
	Floor	Low floor, Middle floor, High floor	N/A
	Total floors	1 to 64	floor
	Building area	21.57 to 376.67	m ²
	Layout structure	Split-level, Single-level, Duplex, Data Not Available	N/A
	Inner area	16.29 to 262.89, Data Not Available	m ²
	Building type	Slab, Slab-Tower Combination, Tower, Bungalow, Data Not Available	N/A
	House orientation	South, East, West, North, Southeast, Southwest, Northeast, Northwest, Multiple Orientations	N/A
	Building structure	Steel-Concrete, Unknown, Frame, Mixed, Brick-Concrete, Steel	N/A
Community Attributes	Decoration condition	YES/NO	Boolean
	Elevator-to-apartment Ratio	2:1 to 20:32	N/A
	Equipped with elevator	YES/NO	Boolean
	Transaction ownership	Commercial Housing, Price-Limited Housing, Demolished and Reconstructed Housing, Affordable Housing, Funded Housing	N/A
	Property age	Over 2 Years, Under 2 Years, Data Not Available	N/A
	Community name	-	N/A

Reference average price	4,127 to 90,139	CNY
Year of construction	2016 to 2022	N/A
Property fee	0.1 to 7.8	CNY/m ² /month
Total number of buildings	1 to 229	Buildings
Total number of apartments	3 to 11,093	Apartments
Longitude	114.014 to 114.626	°E
Latitude	30.305 to 30.895	°N

Note: “N/A” stands for “Not Available” or “Not Applicable”.

Table A.2. VIF of OLS models

Variable	VIF for baseline model	VIF for model I	VIF for model II
Area	1.34	1.316	1.316
Age	1.006	1.006	1.006
Floor	2.04	2.038	2.038
Tot_floor	1.47	1.45	1.45
Decoration	1.062	1.061	1.061
E2A_ratio	1.353	1.352	1.352
Prop_fee	1.719	1.679	1.679
Dis_pri	3.577	2.795	2.795
Dis_mid	1.839	1.754	1.754
Dis_uni	14.936	-	-
Dis_hos	1.541	1.532	1.532
Dis_sub	1.379	1.315	1.315
Dis_aero	1.826	1.803	1.803
Dis_tra	4.527	3.804	3.804
Dis_rail	1.558	1.528	1.528
Dis_road	14.832	-	-
WVIsky	1,490,352.00	2.009	-
WVIhigh	2,277,566.00	-	3.07
WVIlow	244,538.20	1.183	1.911
WVIgrass	104,949.80	1.147	1.266

WVIhard	96,186.21	1.239	1.231
WVItree	1,036,564.00	1.575	2.611
WVIwater	14,818.36	1.1	1.176
WVIroad	38,407.27	1.104	1.259
WVIbarren	45,983.99	1.064	1.191

Table A.3. LM tests for model I and model II

	Model I	Model II
LM test (error)	31,755 ***	31,755***
LM test (lag)	3,281***	3,281***
Robust LM test (error)	28,869***	28,869***
Robust LM test (lag)	394.61***	394.61***

Declaration of Competing Interest

The authors report no declarations of interest.

CRedit authorship contribution statement

Chucaï Peng: Conceptualization, Methodology, Software, Writing - original draft. Yang Xiang: Formal analysis, Visualization. Wenjing Huang: Investigation, Data curation. Yale Feng: Investigation, Data curation. Yongqi Tang: Investigation, Data curation. Filip Biljecki: Writing - review & editing. Zhixiang Zhou: Validation, Funding acquisition, Supervision.

Acknowledgments

This research was funded by the National key R & D Program of China (Grant No. 2023YFF1305202), and the National Natural Science Foundation of China (Grant No. 31770748 and 31870701), and is part of the project Large-scale 3D Geospatial Data for Urban Analytics, which is supported by the National University of Singapore under the Start Up Grant R-295-000-171-133.

References

- Anselin, L. (1988). Lagrange multiplier test diagnostics for spatial dependence and spatial heterogeneity. *Geographical Analysis*, 20, 1 – 17. doi:10.1111/j.1538-4632.1988.tb00159.x.
- Aries, M.B.C., Veitch, J.A., & Newsham, G.R. (2010). Windows, view, and office characteristics predict physical and psychological discomfort. *Journal of Environmental Psychology*, 30, 533 – 541. doi:10.1016/j.jenvp.2009.12.004.
- Badrinarayanan, V., Kendall, A., & Cipolla, R. (2017). SegNet: A deep convolutional encoder-decoder architecture for image segmentation. *IEEE Transactions on Pattern Analysis and Machine Intelligence*, 39, 2481 – 2495. doi:10.1109/TPAMI.2016.2644615.
- Beike Research Institute (2020). Super high-rise residential PK in 19 cities: Wuhan has 10 times more skyscrapers than Beijing [WWW Document]. <https://m.ke.com/kandian/MjAzNzI1OTc=.html?beikefrom=beikehao>. (Accessed 9 January 2022).
- Bi, W., Jiang, X., Li, H., Cheng, Y., Jia, X., Mao, Y., & Zhao, B. (2022). The more natural the window, the healthier the isolated people—A pathway analysis in Xi' an, China, during the COVID-19 pandemic. *International Journal of Environmental Research and Public Health*, 19, 10165. doi:10.3390/ijerph191610165.
- Biljecki, F., & Chow, Y.S. (2022). Global building morphology indicators. *Computers, Environment and Urban Systems*, 95, 101809. doi:10.1016/j.compenvurbsys.2022.101809.

- Bivand, R., Millo, G., & Piras, G. (2021). A review of software for spatial econometrics in R. *Mathematics*, 9, 1276. doi:10.3390/math9111276.
- Bolte, A.-M., Niedermann, B., Kistemann, T., Haunert, J.-H., Dehbi, Y., & Kötter, T. (2024). The green window view index: Automated multi-source visibility analysis for a multi-scale assessment of green window views. *Landscape Ecology*, 39, 71. doi:10.1007/s10980-024-01871-7.
- Bourassa, S.C., Hoesli, M., & Sun, J. (2004). What's in a view? *Environment & Planning A*, 36, 1427 - 1450. doi:10.1068/a36103.
- Cao, Y., & Huang, L. (2023). A study on the impact of small-scale courtyard landscape layouts on spatial oppressiveness in dense high-rise environments. *Sustainability*, 15, 14826. doi:10.3390/su152014826.
- Chang, C., Oh, R.R.Y., Nghiem, T.P.L., Zhang, Y., Tan, C.L.Y., Lin, B.B., ... Carrasco, L.R. (2020). Life satisfaction linked to the diversity of nature experiences and nature views from the window. *Landscape and Urban Planning*, 202, 103874. doi:10.1016/j.landurbplan.2020.103874.
- Chen, L.-C., Papandreou, G., Kokkinos, I., Murphy, K., & Yuille, A.L. (2018). DeepLab: Semantic image segmentation with deep convolutional nets, Atrous convolution, and fully connected CRFs. *IEEE Transactions on Pattern Analysis and Machine Intelligence*, 40, 834 - 848. doi:10.1109/TPAMI.2017.2699184.
- Chung, W.K., Chau, C.K., Masullo, M., & Pascale, A. (2019). Modelling perceived oppressiveness and noise annoyance responses to window views of densely packed residential high-rise environments. *Building and Environment*, 157, 127 - 138. doi:10.1016/j.buildenv.2019.04.042.
- Chung, W.K., Lin, M., Chau, C.K., Masullo, M., Pascale, A., Leung, T.M., & Xu, M. (2022). On the study of the psychological effects of blocked views on dwellers in high dense urban environments. *Landscape and Urban Planning*, 221, 104379. doi:10.1016/j.landurbplan.2022.104379.

- Dai, X., Felsenstein, D., & Grinberger, A.Y. (2023). Viewshed effects and house prices: Identifying the visibility value of the natural landscape. *Landscape and Urban Planning*, 238, 104818. doi:10.1016/j.landurbplan.2023.104818.
- Damigos, D., & Anyfantis, F. (2011). The value of view through the eyes of real estate experts: A Fuzzy Delphi approach. *Landscape and Urban Planning*, 101, 171 – 178. doi:10.1016/j.landurbplan.2011.02.009.
- Domjan, S., Arkar, C., & Medved, S. (2023). Study on occupants' window view quality vote and their physiological response. *Journal of Building Engineering*, 68, 106119. doi:10.1016/j.jobeb.2023.106119.
- Duan, J., Tian, G., Yang, L., & Zhou, T. (2021). Addressing the macroeconomic and hedonic determinants of housing prices in Beijing Metropolitan Area, China. *Habitat International*, 113, 102374. doi:10.1016/j.habitatint.2021.102374.
- Elsadek, M., Liu, B., & Xie, J. (2020). Window view and relaxation: Viewing green space from a high-rise estate improves urban dwellers' wellbeing. *Urban Forestry & Urban Greening*, 55, 126846. doi:10.1016/j.ufug.2020.126846.
- Fan, Z., Zhang, F., Loo, B.P.Y., & Ratti, C. (2023). Urban visual intelligence: Uncovering hidden city profiles with street view images. *Proceedings of the National Academy of Sciences*, 120, e2220417120. doi:10.1073/pnas.2220417120.
- Guo, M.-H., Lu, C.-Z., Hou, Q., Liu, Z., Cheng, M.-M., & Hu, S. (2022). SegNeXt: Rethinking convolutional attention design for semantic segmentation. *Advances in Neural Information Processing Systems*, 35, 1140 – 1156.
- Hamilton, S.E., & Morgan, A. (2010). Integrating lidar, GIS and hedonic price modeling to measure amenity values in urban beach residential property markets. *Computers, Environment and Urban Systems*, 34, 133 – 141. doi:10.1016/j.compenvurbsys.2009.10.007.
- Hasegawa, Y., Lau, S.-K., & Chau, C.K. (2022). Potential mutual efforts of landscape factors to improve residential soundscapes in compact urban cities. *Landscape and Urban Planning*, 227, 104534. doi:10.1016/j.landurbplan.2022.104534.

- Irwin, P., Arcari, C., Hausbeck, J., & Paskewitz, S. (2008). Urban wet environment as mosquito habitat in the upper Midwest. *EcoHealth*, 5, 49 – 57.
doi:10.1007/s10393-007-0152-y.
- Ito, K., & Biljecki, F. (2021). Assessing bikeability with street view imagery and computer vision. *Transportation Research Part C: Emerging Technologies*, 132, 103371. doi:10.1016/j.trc.2021.103371.
- Jim, C.Y., & Chen, W.Y. (2006). Impacts of urban environmental elements on residential housing prices in Guangzhou (China). *Landscape and Urban Planning*, 78, 422 – 434. doi:10.1016/j.landurbplan.2005.12.003.
- Jim, C.Y., & Chen, W.Y. (2009). Value of scenic views: Hedonic assessment of private housing in Hong Kong. *Landscape and Urban Planning*, 91, 226 – 234. doi:10.1016/j.landurbplan.2009.01.009.
- Ko, W.H., Kent, M.G., Schiavon, S., Levitt, B., & Betti, G. (2022). A window view quality assessment framework. *LEUKOS*, 18, 268 – 293.
doi:10.1080/15502724.2021.1965889.
- Ko, W.H., Schiavon, S., Santos, L., Kent, M.G., Kim, H., & Keshavarzi, M. (2023). View access index: The effects of geometric variables of window views on occupants' satisfaction. *Building and Environment*, 234, 110132.
doi:10.1016/j.buildenv.2023.110132.
- Li, D., & Sullivan, W.C. (2016). Impact of views to school landscapes on recovery from stress and mental fatigue. *Landscape and Urban Planning*, 148, 149 – 158.
doi:10.1016/j.landurbplan.2015.12.015.
- Li, J., Hu, Y., & Liu, C. (2020). Exploring the influence of an urban water system on housing prices: Case study of Zhengzhou. *Buildings*, 10, 44.
doi:10.3390/buildings10030044.
- Li, M., Xue, F., Wu, Y., & Yeh, A.G.O. (2022). A room with a view: Automatic assessment of window views for high-rise high-density areas using City information models and deep transfer learning. *Landscape and Urban Planning*, 226, 104505. doi:10.1016/j.landurbplan.2022.104505.

- Li, W., & Samuelson, H. (2020). A new method for visualizing and evaluating views in architectural design. *Developments in the Built Environment*, 1, 100005. doi:10.1016/j.dibe.2020.100005.
- Li, X., Chen, W.Y., & Hin Ting Cho, F. (2020). 3-D spatial hedonic modelling: Environmental impacts of polluted urban river in a high-rise apartment market. *Landscape and Urban Planning*, 203, 103883. doi:10.1016/j.landurbplan.2020.103883.
- Li, X., Li, L., Wang, X., Lin, Q., Wu, D., Dong, Y., & Han, S. (2021). Visual quality evaluation model of an urban river landscape based on random forest. *Ecological Indicators*, 133, 108381. doi:10.1016/j.ecolind.2021.108381.
- Lin, T.-Y., Le, A.-V., & Chan, Y.-C. (2022). Evaluation of window view preference using quantitative and qualitative factors of window view content. *Building and Environment*, 213, 108886. doi:10.1016/j.buildenv.2022.108886.
- Lindemann-Matthies, P., Benkowitz, D., & Hellinger, F. (2021). Associations between the naturalness of window and interior classroom views, subjective well-being of primary school children and their performance in an attention and concentration test. *Landscape and Urban Planning*, 214, 104146. doi:10.1016/j.landurbplan.2021.104146.
- Liu, T., Hu, W., Song, Y., & Zhang, A. (2020). Exploring spillover effects of ecological lands: A spatial multilevel hedonic price model of the housing market in Wuhan, China. *Ecological Economics*, 170, 106568. doi:10.1016/j.ecolecon.2019.106568.
- Long, J., Shelhamer, E., & Darrell, T. (2015). Fully convolutional networks for semantic segmentation. Presented at the proceedings of the IEEE conference on computer vision and pattern recognition (pp. 3431 – 3440).
- Lundberg, S., & Lee, S.-I. (2017). A Unified approach to interpreting model predictions. doi:10.48550/arXiv.1705.07874.
- Luo, J., Zhao, T., Cao, L., & Biljecki, F. (2022). Semantic Riverscapes: Perception and evaluation of linear landscapes from oblique imagery using computer vision.

- Landscape and Urban Planning, 228, 104569.
doi:10.1016/j.landurbplan.2022.104569.
- Luttik, J. (2000). The value of trees, water and open space as reflected by house prices in the Netherlands. *Landscape and Urban Planning*, 48, 161 – 167.
doi:10.1016/S0169-2046(00)00039-6.
- Manski, C.F. (1993). Identification of endogenous social effects: The reflection problem. *The Review of Economic Studies*, 60, 531 – 542. doi:10.2307/2298123.
- Ministry of Housing and Urban-Rural Development of the People’ s Republic of China (2011). *Design code for residential buildings (GB 50096-2011)*. Beijing: China Architecture & Building Press.
- Mistick, K.A., Campbell, M.J., Thompson, M.P., & Dennison, P.E. (2023). Using airborne lidar and machine learning to predict visibility across diverse vegetation and terrain conditions. *International Journal of Geographical Information Science*, 37, 1728 – 1764. doi:10.1080/13658816.2023.2224421.
- Mittal, J., & Byahut, S. (2019). Scenic landscapes, visual accessibility and premium values in a single family housing market: A spatial hedonic approach. *Environment and Planning B: Urban Analytics and City Science*, 46, 66 – 83.
doi:10.1177/2399808317702147.
- Orquin, J.L., & Mueller Loose, S. (2013). Attention and choice: A review on eye movements in decision making. *Acta Psychologica*, 144, 190 – 206.
doi:10.1016/j.actpsy.2013.06.003.
- Park, H., Arai, T., Honma, K., & Imai, K. (2024). View evaluation based on visible quantity and its economic value of high-rise apartment units in the northern area of Seoul. *Journal of Asian Architecture and Building Engineering*, 0, 1 – 23.
doi:10.1080/13467581.2023.2300388.
- Park, J.Y., & Nagy, Z. (2018). Comprehensive analysis of the relationship between thermal comfort and building control research - a data-driven literature review. *Renewable and Sustainable Energy Reviews*, 82, 2664 – 2679.
doi:10.1016/j.rser.2017.09.102.

- Peng, C., Xiang, Y., Chen, L., Zhang, Y., & Zhou, Z. (2023). The impact of the type and abundance of urban blue space on house prices: A case study of eight megacities in China. *Land*, 12, 865. doi:10.3390/land12040865.
- Potrawa, T., & Teterova, A. (2022). How much is the view from the window worth? Machine learning-driven hedonic pricing model of the real estate market. *Journal of Business Research*, 144, 50 – 65. doi:10.1016/j.jbusres.2022.01.027.
- Qiu, W., Zhang, Z., Liu, X., Li, W., Li, X., Xu, X., & Huang, X. (2022). Subjective or objective measures of street environment, which are more effective in explaining housing prices? *Landscape and Urban Planning*, 221, 104358. doi:10.1016/j.landurbplan.2022.104358.
- Quan, W., Zhang, R., Zhang, Y., Li, Z., Wang, J., & Yan, D.-M. (2022). Image inpainting with local and global refinement. *IEEE Transactions on Image Processing*, 31, 2405 – 2420. doi:10.1109/TIP.2022.3152624.
- Raanaas, R.K., Patil, G.G., & Hartig, T. (2012). Health benefits of a view of nature through the window: A quasi-experimental study of patients in a residential rehabilitation center. *Clinical Rehabilitation*, 26, 21 – 32. doi:10.1177/0269215511412800.
- Rossetti, T., Lobel, H., Rocco, V., & Hurtubia, R. (2019). Explaining subjective perceptions of public spaces as a function of the built environment: A massive data approach. *Landscape and Urban Planning*, 181, 169 – 178. doi:10.1016/j.landurbplan.2018.09.020.
- Sander, H.A., & Polasky, S. (2009). The value of views and open space: Estimates from a hedonic pricing model for Ramsey County, Minnesota, USA. *Land Use Policy*, 26, 837 – 845. doi:10.1016/j.landusepol.2008.10.009.
- Schmid, H.-L., & Säumel, I. (2021). Outlook and insights: Perception of residential greenery in multistorey housing estates in Berlin, Germany. *Urban Forestry & Urban Greening*, 63, 127231. doi:10.1016/j.ufug.2021.127231.
- Seo, K., Golub, A., & Kuby, M. (2014). Combined impacts of highways and light rail transit on residential property values: A spatial hedonic price model for Phoenix,

- Arizona. *Journal of Transport Geography*, 41, 53 – 62.
doi:10.1016/j.jtrangeo.2014.08.003.
- Sheng, G.Q., Ingabo, S.N., & Chan, Y.-C. (2024). Evaluating the impact of bird collision prevention glazing patterns on window views. *Building and Environment*, 259, 111657. doi:10.1016/j.buildenv.2024.111657.
- Su, D., Kong, H., Qiao, Y., & Sukkarieh, S. (2021). Data augmentation for deep learning based semantic segmentation and crop-weed classification in agricultural robotics. *Computers and Electronics in Agriculture*, 190, 106418. doi:10.1016/j.compag.2021.106418.
- Sun, M., Han, C., Nie, Q., Xu, J., Zhang, F., & Zhao, Q. (2022). Understanding building energy efficiency with administrative and emerging urban big data by deep learning in Glasgow. *Energy and Buildings*, 273, 112331. doi:10.1016/j.enbuild.2022.112331.
- Sun, M., Zhang, F., Duarte, F., & Ratti, C. (2022). Understanding architecture age and style through deep learning. *Cities*, 128, 103787. doi:10.1016/j.cities.2022.103787.
- Suvorov, R., Logacheva, E., Mashikhin, A., Remizova, A., Ashukha, A., Silvestrov, A., ... Lempitsky, V. (2022). Resolution-robust large mask inpainting with fourier convolutions. Presented at the proceedings of the IEEE/CVF winter conference on applications of computer vision (pp. 2149 – 2159).
- Swietek, A.R., & Zumwald, M. (2023). Visual capital: Evaluating building-level visual landscape quality at scale. *Landscape and Urban Planning*, 240, 104880. doi:10.1016/j.landurbplan.2023.104880.
- Tang, L., Ying, S., Li, L., Biljecki, F., Zhu, H., Zhu, Y., ... Su, F. (2020). An application-driven LOD modeling paradigm for 3D building models. *ISPRS Journal of Photogrammetry and Remote Sensing*, 161, 194 – 207. doi:10.1016/j.isprsjprs.2020.01.019.
- Turan, I., Chegut, A., Fink, D., & Reinhart, C. (2021). Development of view potential metrics and the financial impact of views on office rents. *Landscape and Urban Planning*, 215, 104193. doi:10.1016/j.landurbplan.2021.104193.

- Ulrich, R.S. (1984). View through a window may influence recovery from surgery. *Science*, 224, 420 – 421. doi:10.1126/science.6143402.
- Van Renterghem, T., Vermandere, E., & Lauwereys, M. (2023). Road traffic noise annoyance mitigation by green window view: Optimizing green quantity and quality. *Urban Forestry & Urban Greening*, 88, 128072. doi:10.1016/j.ufug.2023.128072.
- Vásquez, N.G., Felipe, M.L., Pereira, F.O.R., & Kuhnen, A. (2019). Luminous and visual preferences of young children in their classrooms: Curtain use, artificial lighting and window views. *Building and Environment*, 152, 59 – 73. doi:10.1016/j.buildenv.2019.01.049.
- Wang, B., Xu, T., Gao, H., Ta, N., Chai, Y., & Wu, J. (2021). Can daily mobility alleviate green inequality from living and working environments? *Landscape and Urban Planning*, 214, 104179. doi:10.1016/j.landurbplan.2021.104179.
- Wang, Y., & Shaw, D. (2018). The complexity of high-density neighbourhood development in China: Intensification, deregulation and social sustainability challenges. *Sustainable Cities and Society*, 43, 578 – 586. doi:10.1016/j.scs.2018.08.024.
- Wen, H., & Tao, Y. (2015). Polycentric urban structure and housing price in the transitional China: Evidence from Hangzhou. *Habitat International*, 46, 138 – 146. doi:10.1016/j.habitatint.2014.11.006.
- Wen, H., Xiao, Y., & Zhang, L. (2017). School district, education quality, and housing price: Evidence from a natural experiment in Hangzhou, China. *Cities*, 66, 72 – 80. doi:10.1016/j.cities.2017.03.008.
- Wu, C., Du, Y., Li, S., Liu, P., & Ye, X. (2022). Does visual contact with green space impact housing prices? an integrated approach of machine learning and hedonic modeling based on the perception of green space. *Land Use Policy*, 115, 106048. doi:10.1016/j.landusepol.2022.106048.
- Wuhan Municipal Bureau of Statistics (2022). *Wuhan statistical yearbook 2021*.

- Xian, M., Xu, F., Cheng, H.D., Zhang, Y., & Ding, J. (2016). EISeg: Effective interactive segmentation. 2016 23rd international conference on pattern recognition (ICPR). Presented at the 2016 23rd international conference on pattern recognition (ICPR) (pp. 1982 – 1987). doi:10.1109/ICPR.2016.7899927.
- Xie, E., Wang, W., Yu, Z., Anandkumar, A., Alvarez, J.M., & Luo, P. (2021). SegFormer: Simple and efficient design for semantic segmentation with transformers. *Advances in neural information processing systems* (pp. 12077 – 12090). Curran Associates, Inc..
- Xu, G., Yue, Q., Liu, X., & Chen, H. (2024). Investigation on the effect of data quality and quantity of concrete cracks on the performance of deep learning-based image segmentation. *Expert Systems with Applications*, 237, 121686. doi:10.1016/j.eswa.2023.121686.
- Xu, X., Qiu, W., Li, W., Liu, X., Zhang, Z., Li, X., & Luo, D. (2022). Associations between street-view perceptions and housing prices: Subjective vs. objective measures using computer vision and machine learning techniques. *Remote Sensing*, 14, 891. doi:10.3390/rs14040891.
- Xue, C.Q., Gu, Y., & Leung, Y.H. (2022). Waterfront development and planning control: A case study of Victoria dockside in Hong Kong. *Urban Design International*. doi:10.1057/s41289-022-00212-x.
- Yamagata, Y., Murakami, D., Yoshida, T., Seya, H., & Kuroda, S. (2016). Value of urban views in a bay city: Hedonic analysis with the spatial multilevel additive regression (SMAR) model. *Landscape and Urban Planning*, 151, 89 – 102. doi:10.1016/j.landurbplan.2016.02.008.
- Yang, S., Krenz, K., Qiu, W., & Li, W. (2023). The role of subjective perceptions and objective measurements of the urban environment in explaining house prices in greater London: A multi-scale urban morphology analysis. *ISPRS International Journal of Geo-Information*, 12, 249. doi:10.3390/ijgi12060249.
- Yao, T., Lin, W., Bao, Z., & Zeng, C. (2024). Natural or balanced? The physiological and psychological benefits of window views with different proportions of sky, green space, and buildings. *Sustainable Cities and Society*, 104, 105293. doi:10.1016/j.scs.2024.105293.

Yu, J., Lin, Z., Yang, J., Shen, X., Lu, X., & Huang, T.S. (2019). Free-form image inpainting with gated convolution. Presented at the proceedings of the IEEE/CVF international conference on computer vision (pp. 4471 - 4480).